

Transition to a crystalline high-pressure phase in α -GeO₂ at room temperature

J. Haines, J. M. Léger, and C. Chateau

Laboratoire de Physico-Chimie des Matériaux, Centre National de la Recherche Scientifique, 1 Place Aristide Briand,
F-92190 Meudon, France

(Received 19 October 1999)

α -quartz-type GeO₂ was found to undergo a transition to a crystalline phase above 6 GPa at room temperature from *in situ*, angle-dispersive, x-ray-diffraction measurements. There was no evidence of amorphization, although this phase is poorly crystallized. Hydrostatic conditions play an important role in the crystallization process. The crystal structure of this high-pressure form of GeO₂ was found to be monoclinic, space group $P2_1/c$, $Z=6$ and is built up of 3×2 kinked chains of edge-sharing GeO₆ octahedra. This phase is 45% denser than α -quartz-type GeO₂ and 1% less dense than the rutile-type phase and is metastable from ambient pressure up to at least 50 GPa at room temperature. Upon heating this monoclinic phase at pressures up to 22 GPa, rutile-type GeO₂ is formed, whereas at 43 GPa a mixture of the CaCl₂-type and Fe₂N-type phases is obtained.

I. INTRODUCTION

There has been considerable interest in pressure-induced amorphization since the phenomenon was first identified in Ice-Ih.¹ Pressure-induced amorphization has also been reported to occur in α -quartz SiO₂ (Ref. 2) and related quartz-like materials, such as α -GeO₂ (Refs. 3–11), PON,¹² and berlinite-type ABO₄ ($A = \text{Al, Ga}$, $B = \text{P, As}$) compounds.^{13–18} Some recent studies indicate that in the case of several berlinites, the high-pressure phase may in fact be crystalline.^{14–18} The coexistence of crystalline and amorphous phases has been reported for α -quartz SiO₂ compressed under nonhydrostatic conditions.¹⁹ The high-pressure behavior of quartz-type α -GeO₂ has been investigated by a large variety of experimental techniques including x-ray diffraction, x-ray absorption, Brillouin scattering and infrared and Raman spectroscopy.^{3–11, 20–23} A transition was found to occur above 6 GPa at which the germanium coordination number increases from four to six.²⁰ In several studies the high-pressure phase has been reported to be amorphous;^{3–11} however, others^{21, 22} indicate that the phase is crystalline for which the structure remains unknown. It is possible that depending on the starting material and the experimental conditions either an amorphous or a crystalline phase may be formed. Recent work²⁴ on FePO₄ indicated that both a crystalline and an amorphous phase are formed simultaneously above the phase transition. In the present study, α -GeO₂ was found to transform to a crystalline phase with a monoclinic structure both under hydrostatic and nonhydrostatic conditions and no evidence was found for pressure-induced amorphization.

II. EXPERIMENT

High-pressure experiments on quartz-type α -GeO₂ (Produits Touzart & Matignon, purity 99.999%) were performed in a diamond anvil cell (DAC). The phase purity of the sample was 99.4% based on data acquired on a standard diffractometer using copper $K\alpha$ radiation with the remaining material being in the rutile form. The cell constants of

α -quartz-type GeO₂ (space group $P3_121$, $Z=3$) were found to be $a=4.9853(1)$ Å and $c=5.6471(2)$ Å. Heating the sample for 10 h at 1070 °C followed by quenching increased the phase purity to more than 99.9%. The widths of the x-ray-diffraction lines of the α -GeO₂ sample are consistent with a crystallite size of the order of 80 nm. Samples were loaded in the 150–200 μm diameter holes of inconel or stainless steel gaskets preindented to a thickness of 100–120 μm along with a small amount of ruby powder as a pressure calibrant. Experiments were performed using the following media: 16:3:1 methanol:ethanol:H₂O, silicone grease and no medium. In certain runs, titanium carbide was added to absorb laser radiation for sample heating. Laser heating was performed using a 50 W Nd-YAG laser. The sample temperature was not measured, but was estimated to be over 1000 °C based on the visible emission observed. Laser heating experiments at high pressure were also performed on GeO₂ glass and on rutile-type GeO₂ (space group $P4_2/mnm$, $Z=2$, $a=4.3966(1)$ Å, $c=2.8626(1)$ Å). Both materials were prepared from α -GeO₂. The glass was prepared at 1200 °C and ambient pressure and the rutile-type phase at 3.0 GPa and 585 °C in a belt-type apparatus.²⁵

Angle-dispersive, x-ray-diffraction patterns were obtained on an imaging plate placed at between 113.65 and 147.26 mm from the sample using zirconium-filtered molybdenum radiation from a microfocus tube. An x-ray capillary optic was used giving a beam diameter of 100 μm . Exposure times were typically of between 24–60 h. A DAC in which the rear diamond was mounted over a 16° wide slit allowing access to an angular range $4\theta=80^\circ$ was used for these experiments. Pressures were measured based on the shifts of the ruby R_1 and R_2 fluorescence lines.²⁶ Exposures on the materials recovered in the gasket after the various experiments were obtained using the same installation with sample to plate distances of 106.73–142.64 mm.

The observed intensities on the imaging plates were integrated as a function of 2θ in order to give conventional, one-dimensional diffraction profiles. Profile fitting and simulations of the powder diffraction pattern obtained after a 96 h

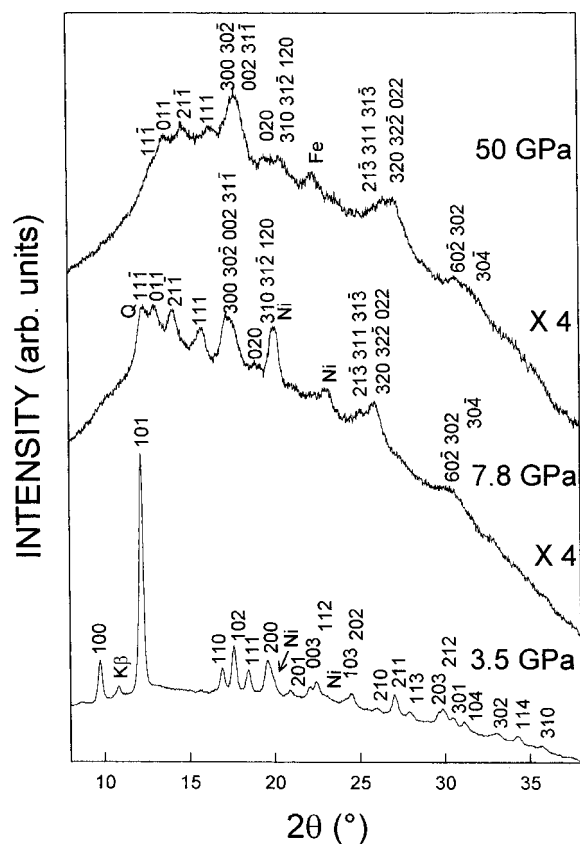


FIG. 1. X-ray-diffraction patterns ($\lambda = 0.71073 \text{ \AA}$) of GeO_2 as a function of pressure. The data for the α -quartz-type phase at 3.5 GPa and the monoclinic phase at 7.8 GPa were obtained under hydrostatic conditions, whereas for the data for the monoclinic phase at 50 GPa, the pressure-transmitting medium was solid. The principal lines due to GeO_2 are indexed. Additional lines are identified: $K\beta$ =strongest line due to $K\beta$ radiation, Ni=nickel (gasket), Fe=iron (gasket), and Q =strongest line from the α -quartz-type phase persisting above the high-pressure phase transition.

exposure on a sample in a gasket were performed using the program FULLPROF.²⁷ All figures in parentheses refer to estimated standard deviations (e.s.d.).

III. RESULTS AND DISCUSSION

A. High-pressure phase transition

Pronounced changes to the diffraction pattern of α - GeO_2 were observed above 6 GPa, Fig. 1. The diffraction lines from the initial α -quartz-type phase were found to disappear and several new diffraction lines were observed indicating the formation of a crystalline high-pressure phase. The transparent powder grains were found to become translucent at the phase transition as had previously been observed.⁷ These changes can be interpreted in terms of the breaking up of the crystallites at the phase transition. This is supported by the observation that the full width at half maximum (FWHM) of the x-ray-diffraction lines doubles at the phase transition under hydrostatic conditions. No further transition was observed up to 50 GPa at room temperature. Upon decompression, this phase could be retained down to ambient pressure.

This transition was found to occur under hydrostatic conditions in 16:3:1 methanol:ethanol: H_2O and under nonhydro-

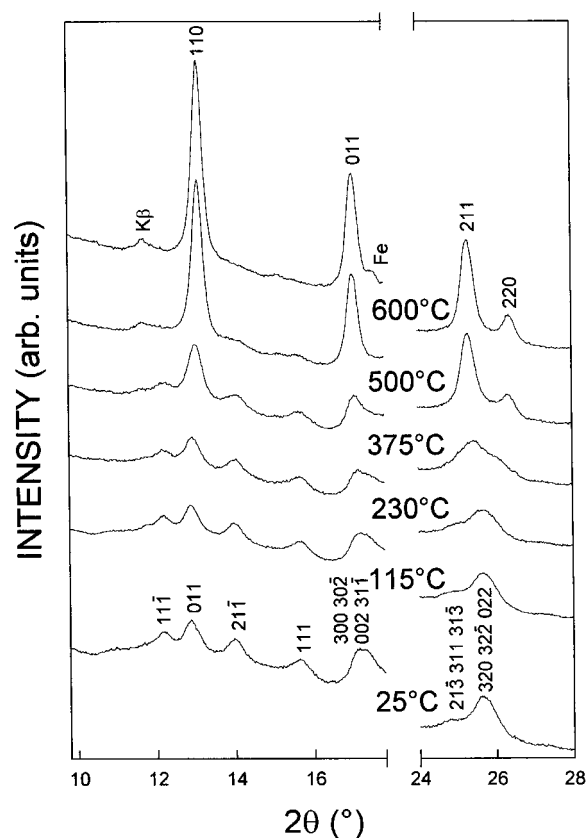


FIG. 2. X-ray-diffraction patterns ($\lambda = 0.71073 \text{ \AA}$) under ambient conditions obtained as a function of the temperature at which monoclinic GeO_2 was annealed followed by quenching at ambient pressure. The sample had been compressed to a maximum pressure of 18.1 GPa in 16:3:1 methanol:ethanol: H_2O . The principal lines due to GeO_2 are indexed in the 25 °C pattern corresponding to the $P2_1/c$ phase and in that after heating at 600 °C corresponding to the rutile-type phase. Additional lines are identified: $K\beta$ =strongest line due to $K\beta$ radiation and Fe=iron from the gasket.

static conditions in either silicone grease or without a pressure-transmitting medium. Under nonhydrostatic conditions, a significant quantity of the α -quartz-type phase continued to be present above 9 GPa and the diffraction lines broadened to an even greater extent. The FWHM of the diffraction lines arising from a sample without a pressure-transmitting medium compressed to 20 GPa over a 20 min time frame and then quenched approached 1° in 2θ . In contrast, the FWHM of lines of a sample slowly compressed under hydrostatic conditions to a maximum pressure of 9.2 GPa were of the order of 0.5° . In both cases the relative intensities of the diffraction lines were similar; however, their positions were shifted by between 0.04 – 0.15° .

B. High-temperature transition at ambient pressure

A series of high-temperature experiments were performed on the quenched high-pressure phase in the gasket, Fig. 2. The sample was heated in a furnace for four hours and quenched between x-ray exposures. The positions and intensities of the diffraction lines were found to tend gradually towards those of the rutile-type phase with each treatment at a progressively higher temperature. The pure rutile-type phase was obtained by 600 °C. No changes were observed

upon further heating to 920 °C. This behavior is very different from that of GeO₂ glass, which was found to completely transform to quartz-type GeO₂ below 600 °C, and from those of pressure-amorphized samples, which transformed to a mixture of the quartz-type and rutile-type phases below 600 °C (Ref. 10). X-ray absorption experiments²⁰ indicated that whereas in GeO₂ glass, the coordination number increased from 4 to 6 reversibly with pressure, in α -GeO₂ the increase in coordination number is irreversible. In the latter case, the high-pressure phase was found to be crystalline.²¹ It can therefore be expected that crystalline material recovered from high pressure in which the germanium is in sixfold coordination would transform to the rutile-type phase upon heating, whereas amorphous material containing fourfold coordinated germanium would transform to the quartz-type phase. In the present study, no α -GeO₂ was formed. This is taken as an indication that no amorphous material was present in the sample and that the entire sample underwent a crystalline-crystalline phase transition to the rutile-type phase. The gradual changes in intensity and position of the diffraction lines is interpreted in terms of the progressive displacement of germanium atoms from their positions in the new phase to those in the rutile-type phase with the germanium atoms remaining in sixfold coordination.

C. Structure of the high-pressure phase

The broad diffraction lines of the high-pressure phase ruled out the use of automatic indexing programs in order to determine the unit cell. The positions of selected relatively intense diffraction lines of the high-pressure phase at $2\theta > 16^\circ$ were found to be similar to those observed for both tetragonal, rutile-type and hexagonal Fe₂N-type (space group $P6_3/mmc$, $Z=1$) (Ref. 28) GeO₂. These structures are based on a hexagonal close packed (hcp) oxygen array in which one half of the octahedral sites are occupied by cations. In the rutile structure, the oxygen array is distorted and the cations are ordered, whereas in the Fe₂N structure the octahedral sites are occupied randomly. In the diffraction pattern of Fe₂N-type GeO₂ (Ref. 28), no diffraction lines are observed below 17°. Based on the similarities in the higher angle part of the diffraction pattern, the hypothesis of a hcp oxygen array was adopted, while the presence of strong reflections between 12° and 16° was taken as an indication of cation ordering. A search was thus made in the literature for structures based on a hcp anion array with an ordered occupation of one half of the octahedral sites. A large number of observed and theoretical structures were tested as models; however, only one solution could adequately reproduce the experimental line positions. This structural model is based on the (3×2) -kinked $P2_1/c$ structure type recently described by Teter *et al.*²⁹ It was also possible to index the diagram of a phase obtained upon compression of α -quartz SiO₂ to 213 GPa under nonhydrostatic conditions using this structural model.^{19,29} In addition, calculations²⁹ indicate that α -quartz can undergo a diffusionless transformation to this structure. In the present case, this could explain the formation of a (3×2) -kinked $P2_1/c$ phase upon compression of α -GeO₂ at room temperature, rather than the stable rutile-type phase, which is readily obtained upon heating. Simulation of the experimental x-ray-diffraction pattern using this model struc-

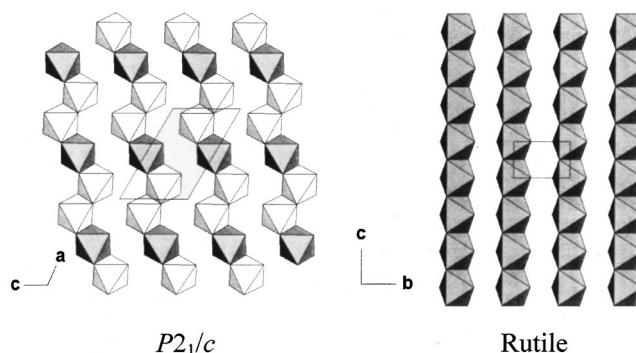


FIG. 3. Polyhedral representations of a layer of the (3×2) -kinked $P2_1/c$ structure and the corresponding layer of the rutile-type structure. Shaded and unshaded polyhedra in the monoclinic structure correspond to octahedra centered by Ge1 and Ge3, respectively.

ture produced good agreement except for the intensities of the diffraction lines that were found to tend towards those of the rutile-type phase at high temperature. The experimental intensities of these lines were found to be greater than those calculated, which was taken to be an indication that a certain proportion of the cations were already in rutile-like sites. The presence of a certain degree of cation disorder could also partially account for the broad diffraction lines observed even under hydrostatic conditions.

Three potential transformation pathways between the monoclinic (m) (3×2) -kinked $P2_1/c$ structure and the tetragonal (t) rutile structure, Fig. 3, involving cation displacements can readily be envisaged. One possibility, involving the following cell relationships: $\mathbf{a}_m = -3\mathbf{c}_t$, $\mathbf{b}_m = -\mathbf{a}_t$, $\mathbf{c}_m = \mathbf{a}_t + \mathbf{c}_t$, would require a shift of 1/3 of the cations by 1/2 along \mathbf{b}_m and a shear of the unit cell. In this case, the straight chains of the rutile-type structure would be constructed by linking the units composed of two edge-sharing octahedra in the $P2_1/c$ structure. A second possibility with a different set of cell relationships: $\mathbf{a}_m = 3/2(\mathbf{a}_t + \mathbf{c}_t)$, $\mathbf{b}_m = -\mathbf{a}_t$, $\mathbf{c}_m = -\mathbf{a}_t + \mathbf{c}_t$, involves a shift of the cations in every second unit cell in the \mathbf{a} direction by 1/2 along \mathbf{b}_m again with a shear of the unit cell. This model implies passage via a triclinic (tr) cell obtained as follows from the monoclinic cell: $\mathbf{a}_{tr} = 2\mathbf{a}_m$, $\mathbf{b}_{tr} = \mathbf{b}_m$, $\mathbf{c}_{tr} = \mathbf{c}_m$. The straight chains of the rutile-type structure would thus be constructed by linking the units composed of three edge-sharing octahedra in the $P2_1/c$ structure. A third possibility also involves passage via a $(2\mathbf{a}_m, \mathbf{b}_m, \mathbf{c}_m)$ triclinic intermediate and the corresponding cell relationships are as follows: $\mathbf{a}_m = -3/2(\mathbf{a}_t + \mathbf{c}_t)$, $\mathbf{b}_m = -\mathbf{a}_t$, $\mathbf{c}_m = -2\mathbf{c}_t$. In this case, the straight chains would form along \mathbf{c}_m .

The simpler monoclinic case was adopted in attempts to simulate the observed x-ray-diffraction pattern of GeO₂. It was found that if 9% of the cations are shifted to rutile-type positions, a good fit to the observed intensities could be obtained. This was done by partially occupying the $2d$ Wyck-off sites (occupancy=0.26) and reducing the occupancy of the $2b$ sites to 0.74, thus introducing a degree of cation disorder. The $2d$ site in the (3×2) -kinked $P2_1/c$ structure is normally unoccupied. The transformation to the rutile-type structure involves a shift of the germanium atoms from the $2b$ site to the $2d$ sites, while the other germanium atoms

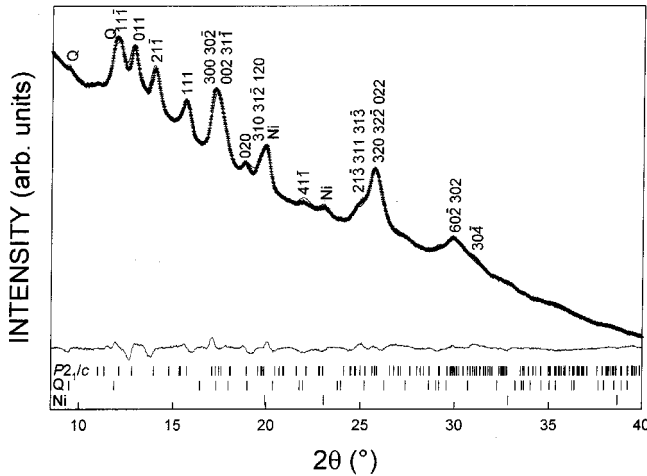


FIG. 4. Experimental data (+) for a sample of GeO_2 recovered at ambient after compression to a maximum pressure of 9.2 GPa in 16:3:1 methanol:ethanol: H_2O and calculated profile (solid line) using the $P2_1/c$ structural model with the values given in Table I. The difference profile is on the same scale. Vertical bars indicate the calculated positions of the diffraction lines of the $P2_1/c$ phase, the remaining α -quartz-type phase (Q), and nickel from the gasket (Ni).

remain on $4e$ sites. The present results indicate that there is a degree of cation disorder in the phase recovered after compression and that at the transition, a proportion of the germanium atoms are placed in the octahedral sites normally occupied in the rutile-type structure. This structural model with a degree of cation disorder was used to fit the experimental data obtained for the high-pressure phase, Fig. 4. The data from sample compressed under hydrostatic conditions to a maximum pressure of 9.2 GPa was used for the profile fitting procedure as line broadening was the least pronounced. It was not possible to refine the structure of the $P2_1/c$ phase due to width of the diffraction lines and the large number of free atomic coordinates. Profile fitting was thus performed with all atomic positions fixed to the values calculated for silica,²⁹ except for the germanium atoms on the $4e$ sites. These germanium positions, the cell constants, and linewidth parameters were varied along with the scale factors for this phase, α -quartz-type GeO_2 (7% of the sample) and nickel from the gasket for which all other parameters were fixed. The Ge atoms on the $4e$ sites were found to shift only slightly from the positions calculated for silica. The following agreement factors were obtained, $R_p = 12.5\%$, $R_{wp} = 12.6\%$, $R_{\text{Bragg}} = 6.5\%$, and the structural data are given in Table I. Similar agreement factors could also be obtained using the second and third models discussed above using triclinic cells doubled along the \mathbf{a} direction with the introduction of cation disorder. There is some supporting evidence for the second model from the line shifts of some peaks at high temperature. All these solutions represent states along transition pathways between the ordered $P2_1/c$ structure and rutile. It is likely that there is competition between these three cation disordering mechanisms and that all three are active.

D. Phase stability in GeO_2

The ratios of relative volumes at ambient pressure, V_0/V_{0Q} , of the various six-coordinated GeO_2 phases,

TABLE I. Structural data used to simulate the diffraction pattern of monoclinic GeO_2 under ambient conditions: space group $P2_1/c$, $Z=6$, $a=8.285(3)$ Å, $b=4.320(1)$ Å, $c=5.410(3)$ Å, and $\beta=119.94(4)^\circ$.

Atom	Site	x	y	z	Occupancy
Ge1	$2b$	1/2	0	0	0.74
Ge2	$2d$	1/2	1/2	0	0.26
Ge3	$4e$	0.160	0.521	0.977	1.00
O1	$4e$	0.054	0.243	0.651	1.00
O2	$4e$	0.721	0.242	0.186	1.00
O3	$4e$	0.387	0.237	0.660	1.00

$P2_1/c$, Fe_2N , and rutile with respect to the α -quartz-type phase (Q) are as follows: 0.690, 0.686, and 0.683. The $P2_1/c$ phase is thus 45% denser than the α -quartz-type phase and 0.6% and 1.0% less dense than the Fe_2N - and the rutile-type phases, respectively. The very similar densities observed for the $P2_1/c$, Fe_2N - and rutile-type phases arise from the fact that the germanium coordination number is 6, as opposed to 4 in the low-density, α -quartz-type phase, and that the oxygen sublattice is hcp or distorted hcp in all three structures. The possible relationships between the $P2_1/c$ and the rutile-type are given in the previous section and both can readily be identified as cation-ordered superstructures of the Fe_2N -type. The cell constants of hexagonal (h) Fe_2N -type GeO_2 at ambient pressure are $a=2.729$ Å and $c=4.312$ Å (Ref. 28). Comparison with the cell constants of the $P2_1/c$ phase, Table I, yields the following relationship between the unit cells: $\mathbf{a}_m = 3\mathbf{a}_{1h}$, $\mathbf{b}_m = \mathbf{c}_h$, and $\mathbf{c}_m = 2\mathbf{a}_{2h}$ (note that the monoclinic β angle in the $P2_1/c$ phase is very close to 120°). The corresponding relationship between the rutile- and Fe_2N -type structures are as follows: $\mathbf{a}_{1r} = -\mathbf{c}_h$, $\mathbf{a}_{2r} = \mathbf{a}_{1h} + \mathbf{a}_{2h}$ and $\mathbf{c}_r = \mathbf{a}_{1h}$. The anion sublattice is much less distorted from hexagonal symmetry in the $P2_1/c$ structure. As cation displacement is required for transformations between these three structures, thermal activation is required.

The rutile-type phase is stable at ambient pressure and temperature and transforms to the quartz-type phase above 1024–1040 °C (Ref. 3). The $P2_1/c$ structure found in the present study and the Fe_2N -type phase, which was prepared from vitreous GeO_2 between 25 and 30 GPa at high temperature,^{28,30} can be retained as metastable phases under ambient conditions. An additional phase, for which the structure is also based on a hcp oxygen sublattice with germanium occupying one half of the octahedral sites, is known. The rutile-type phase has been found to undergo a second-order transition to an orthorhombic CaCl_2 -type phase, space group $Pnmm$ $Z=2$, at 26.7 GPa and ambient temperature.²⁵

Laser heating experiments were performed to investigate the relative stabilities of the various six-coordinated structures at high pressure. α -quartz-type GeO_2 , the glass phase and the rutile-type phase were used as starting materials. The $P2_1/c$ phase, obtained above 6 GPa from the α -quartz-type phase, was found to transform to the rutile-type phase when heated at pressures up to 22 GPa. Heating the $P2_1/c$ phase at 43 GPa yielded a mixture of the CaCl_2 -type phase, the Fe_2N -type phase and some untransformed material. A mixture of the CaCl_2 -type and Fe_2N -type phases was also ob-

tained upon heating the glass at 43 GPa. A small amount of the Fe_2N -type phase was obtained upon heating the CaCl_2 -type phase (rutile-type starting material) at 44 GPa. Reheating the above samples at pressures below 25 GPa yielded the rutile-type phase, otherwise the Fe_2N -type phase is retained down to ambient pressure. Trace germanium metal was detected in the samples containing the Fe_2N -type phase after laser heating at high pressure indicating that a small amount of the GeO_2 was reduced. The strongest diffraction line of germanium was also present in the diffraction pattern obtained by Liu *et al.*²⁸ for GeO_2 after laser heating. Nonstoichiometry may play a role in stabilizing the disordered Fe_2N structure.

The cell constants of the CaCl_2 -type phase at 43 GPa are $a=4.260(3)$ Å, $b=4.109(4)$ Å, and $c=2.768(4)$ Å, while those of the Fe_2N -type phase are $a=2.600(3)$ Å and $c=4.095(9)$ Å. The volume of the Fe_2N -type phase is 1% lower than that of the CaCl_2 -type phase at 43 GPa and 0.3% lower at 28 GPa. As the CaCl_2 -type phase is only present above 26.7 GPa (Ref. 25), it is apparent that its volume is always greater than that of the Fe_2N -type phase. These results are in agreement with previous work³⁰ that indicated although the Fe_2N -type phase is less dense than the rutile-type phase at ambient pressure, it is more compressible. If the germanium dioxide remained stoichiometric in the present study, then the Fe_2N -type structure is stable at high pressure and the CaCl_2 -type structure is metastable. The results of this work indicate that the rutile-type phase is stable below 25 GPa and that the $P2_1/c$ phase is metastable from ambient pressure over the entire pressure range investigated.

E. Pressure-induced amorphization

The present results bring into question the existence of a pressure-induced amorphous phase in GeO_2 . It is obvious from the present study that under certain experimental conditions (i.e., severe nonhydrostatic stress) the diffraction

lines of the high-pressure phase will be so broad that the sample may appear “x-ray amorphous.” There is evidence, however, that a distinct amorphous phase may exist. An infrared study³ indicated that the increase in germanium coordination number was reversible in samples of $\alpha\text{-GeO}_2$ compressed to 30 GPa. Reversible amorphization was also observed by x-ray diffraction.⁶ In another study,⁵ the bulk density of the compressed sample was much closer to that of $\alpha\text{-GeO}_2$ than that of the $P2_1/c$ phase. Samples compressed up to 20 GPa have also been reported to partially revert to $\alpha\text{-GeO}_2$ upon heating at ambient pressure.¹⁰ The behavior described in the present study is distinct. The phase transition was found to be irreversible in all cases, even when the sample was compressed to a maximum pressure of 9.2 GPa, and was observed under hydrostatic and nonhydrostatic conditions and upon slow and rapid compression. The new crystalline phase is only 1% less dense than rutile and it transforms entirely to the rutile-type phase upon heating at ambient pressure. These differences in reported behavior indicate that the competition between crystallization and amorphization is highly sensitive to the origin and nature of the various samples studied.

IV. CONCLUSIONS

$\alpha\text{-GeO}_2$ was found to transform to a crystalline phase above 6 GPa at room temperature. There was no evidence for pressure-induced amorphization. This phase has a monoclinic, crystal structure, space group $P2_1/c$ $Z=2$, composed of (3×2) -kinked chains of GeO_6 octahedra. No pressure-temperature region of stability was identified for this phase, which is metastable at room temperature from ambient pressure up to 50 GPa. This phase transformed to the stable rutile-type phase when heated at pressures up to 22 GPa. A mixture of the CaCl_2 -type and Fe_2N -type phases was obtained upon heating this $P2_1/c$ phase at 43 GPa.

¹O. Mishima, L. D. Calvert, and E. Whalley, *Nature (London)* **310**, 393 (1984).

²R. J. Hemley, A. P. Jephcoat, H. K. Mao, L. C. Ming, and M. H. Manghnani, *Nature (London)* **334**, 52 (1988).

³M. Madon, Ph. Gillet, Ch. Julien, and G. D. Price, *Phys. Chem. Miner.* **18**, 7 (1991).

⁴G. H. Wolf, S. Wang, C. A. Herbst, D. J. Durben, W. F. Oliver, K. C. Kang, and K. Halvorson, in *High-Pressure Research: Applications to Earth and Planetary Sciences*, edited by Y. Syono and M. H. Manghnani (Terra Scientific, Tokyo and American Geophysical Union, Washington, DC, 1992), p. 503.

⁵T. Yamanaka, T. Shibata, S. Kawasaki, and S. Kume, in *High-Pressure Research: Applications to Earth and Planetary Sciences*, edited by Y. Syono and M. H. Manghnani (Ref. 4), p. 493.

⁶M. S. Somayazulu, N. Garg, S. M. Sharma, and S. K. Sikka, *Pramana, J. Phys.* **43**, 1 (1994).

⁷S. Kawasaki, O. Ohtaka, and T. Yamanaka, *Phys. Chem. Miner.* **20**, 531 (1994).

⁸N. Suresh, G. Jyoti, S. C. Gupta, S. K. Sikka, Sangeeta, and S. C.

Sabharwal, *J. Appl. Phys.* **76**, 1530 (1994).

⁹S. Kawasaki, *J. Mater. Sci. Lett.* **15**, 1860 (1996).

¹⁰S. Kawasaki, S. Kume, and E. Ito, *J. Mater. Sci. Lett.* **15**, 261 (1996).

¹¹M. Akaogi, T. Suzuki, R. Kojima, T. Honda, E. Ito, and I. Nakai, *Geophys. Res. Lett.* **25**, 3635 (1998).

¹²J. M. Léger, J. Haines, L. S. de Oliveira, C. Chateau, A. Le Sauze, R. Marchand, and S. Hull, *J. Phys. Chem. Solids* **60**, 145 (1999).

¹³M. B. Kruger and R. Jeanloz, *Science* **249**, 647 (1990).

¹⁴Ph. Gillet, J. Badro, B. Varrel, and P. F. McMillan, *Phys. Rev. B* **51**, 11 262 (1995).

¹⁵J. P. Itié, T. Tinoco, A. Polian, G. Demazeau, S. Matar, and E. Philippot, *High Press. Res.* **14**, 269 (1996).

¹⁶H. Sowa and H. Ahsbahs, *Z. Kristallogr.* **211**, 96 (1996).

¹⁷J. Badro, J. P. Itié, A. Polian, and Ph. Gillet, *J. Phys. IV* **7**, C2-987 (1997).

¹⁸J. Badro, Ph. Gillet, P. F. McMillan, A. Polian, and J. P. Itié, *Europhys. Lett.* **40**, 533 (1997).

¹⁹K. J. Kingma, H. K. Mao, and R. J. Hemley, *High Press. Res.* **14**, 363 (1996).

- ²⁰J. P. Itié, A. Polian, G. Calas, J. Petiau, A. Fontaine, and H. Tolentino, *Phys. Rev. Lett.* **63**, 398 (1989).
- ²¹F. Vannereau, J. P. Itié, A. Polian, G. Calas, J. Petiau, A. Fontaine, and H. Tolentino, *High Press. Res.* **7**, 372 (1991).
- ²²L. Liu and T. P. Mernagh, *High Temp.-High Press.* **24**, 13 (1992).
- ²³J. Glinnemann, H. E. King, Jr., H. Schulz, Th. Hahn, S. J. La Placa, and F. Dacol, *Z. Kristallogr.* **198**, 177 (1992).
- ²⁴M. P. Pasternak, G. Kh. Rozenberg, A. P. Milner, M. Amanowicz, T. Zhou, U. Schwarz, K. Syassen, R. D. Taylor, M. Hanfland, and K. Brister, *Phys. Rev. Lett.* **79**, 4409 (1997).
- ²⁵J. Haines, J. M. Léger, C. Chateau, R. Bini, and L. Ulivi, *Phys. Rev. B* **58**, R2909 (1998).
- ²⁶H. K. Mao, J. Xu, and P. M. Bell, *J. Geophys. Res. B* **91**, 4673 (1986).
- ²⁷J. Rodríguez-Carvajal (unpublished).
- ²⁸L. Liu, W. A. Bassett, and J. Sharry, *J. Geophys. Res.* **83**, 2301 (1978).
- ²⁹D. M. Teter, R. J. Hemley, G. Kresse, and J. Hafner, *Phys. Rev. Lett.* **80**, 2145 (1998).
- ³⁰L. C. Ming and M. H. Manghnani, *Phys. Earth Planet. Inter.* **33**, 26 (1983).